Highly Efficient Utilization of Hydrogen Peroxide for Selective Oxygenation of Alkanes Catalyzed by Diiron-Substituted Polyoxometalate Precursor

Noritaka Mizuno,* Chika Nozaki, Ikuro Kiyoto, and Makoto Misono

Contribution from the Department of Applied Chemistry, Graduate School of Engineering, The University of Tokyo, Hongo, Bunkyo-ku, Tokyo 113-8656, Japan

Received January 2, 1998. Revised Manuscript Received May 15, 1998

Abstract: The Keggin-type iron-substituted polyoxometalates have been used as catalysts for the oxygenation of alkanes in homogeneous reaction media using hydrogen peroxide as an oxygen donor. The efficiency and activity for the utilization of hydrogen peroxide greatly depended on the iron centers and diiron-substituted $[\gamma\text{-}SiW_{10}\{Fe(OH_2)\}_2O_{38}]^{6-}$ showed the highest efficiency of hydrogen peroxide utilization and conversion. Such a structure dependency of the catalysis is significant, and the remarkable catalytic performance of diiron-substituted polyoxometalate may be related to the catalysis by methane monooxygenase. It is remarkable that the efficiency of hydrogen peroxide utilization to oxygenated products reached up to ca. 100% for the oxygenation of cyclohexane catalyzed by diiron-substituted $[\gamma\text{-}SiW_{10}\{Fe(OH_2)\}_2O_{38}]^{6-}$ polyoxometalate. Not only cyclohexane but also *n*-hexane, *n*-pentane, and adamantane were catalytically oxygenated with high efficiency of hydrogen peroxide utilization. It was also suggested that diiron-substituted polyoxometalate was stable under the conditions used and in the presence of hydrogen peroxide.

Introduction

Catalytic oxygenation is used for the conversion of petroleum-derived hydrocarbons to commodities as well as in the manufacture of fine chemicals. In the bulk chemical industry, classical processes that are environmentally unacceptable have been largely supplanted by cleaner, catalytic alternatives. Yet, stoichiometric (noncatalytic) oxygenation is still widely used, and large amounts of byproducts (particularly salts) are formed in the fine chemicals industry. These oxygenation processes require new catalytic, low-salt technologies.[1−3]

Among hydrocarbons, the oxygenation of alkanes has attracted much attention because they are abundant as resources and low in reactivities as feedstocks.[4−6] With respect to the oxidants, fine chemical production allows the choice of various oxygen donors such as peroxides. Among them, hydrogen peroxide is a preferable oxidant because of the simplicity of handling, the environmentally friendly nature of coproduct (water), the high oxygen atom efficiency, and the versatility.[1−3,7] In these contexts, the development of efficient catalysts for the oxygenation of alkanes is very attractive. However, to date, the efficiency of hydrogen peroxide utilization to selective oxygenates was less than 80%, due to the decomposition to molecular oxygen and water.[2,7−12]

Active oxygen transfer agents may be peroxometal or oxometal species formed by the heterolytic cleavage of hydrogen peroxide. Mo^{6+}, W^{6+}, and Ti^{4+} with d^0 configurations favor peroxometal species, and Cr^{5+}, Cr^{3+}, Co^{3+}, and Fe^{3+} favor oxometal species. In fact, iron and manganese porphyrins form high-valent, highly active metal oxo species, leading to the effective hydroxylation of alkanes.

We focused on iron, which is vital to every life-form on Earth, fulfilling biological functions in oxygen transport and catalysis.[13,14] Diiron-containing hemerythrin, ribonucleotide reductase, and methane monooxygenase are the prominent examples of the redox-active enzymes. The active site of methane monooxygenase has already been shown to have a μ-hydroxodiiron structure.[15] Therefore, oxidation catalysis by oxo-bridged di- or triiron metal complexes is a research field important for the development of new catalytic systems and understanding the mechanism of action of iron-containing biomolecules.[12,16−31]

(1) Sheldon, R. A. *Top. Curr. Chem.* **1993**, *164*, 23−43.
(2) Sobkowiak, A.; Tung, H.; Sawyer, D. T. *Prog. Inorg. Chem.***1992**, *40*, 291−352.
(3) Hill, C. L.; Prosser-McCartha, C. M. *Coord. Chem. Rev.* **1995**, *143*, 407−455.
(4) Hill, C. L. *Activation and Functionalization of Alkanes*; Wiley: New York, 1989; pp 243−279.
(5) Crabtree, R. H. *Chem. Rev.* **1995**, *95*, 987−1007.
(6) Okuhara, T.; Mizuno, N.; Misono, M. *Adv. Catal.* **1996**, *41*, 113−252.
(7) Knops-Gerrits, P.; Vos, D. D.; Thibault-Starzyk, F.; Jacobs, P. A. *Nature* **1994**, *369*, 543−546.
(8) Clerici, M. G. *Appl. Catal.* **1991**, *68*, 249−261.
(9) Mizuno, N.; Hirose, T.; Tateishi, M.; Iwamoto, M. *J. Mol. Catal.* **1994**, *88*, L125−L131.
(10) Ménage, S.; Vincent, J. M.; Lambeaux, C.; Fontecave, M. *J. Chem. Soc., Dalton Trans.* **1994**, 2081−2084.
(11) Barton, D. H. R.; Hu, B.; Taylor, D. K.; Rojas Wahl, R. V. *Tetrahedron Lett.* **1996**, *37*, 1133−1136.
(12) Nam, W.; Valentine, J. S. *New J. Chem.* **1989**, *13*, 677−682.
(13) Powell, A. K. *Struct. Bonding* **1992**, *88*, 1−225.
(14) Holm, R. H.; Kennepohl, P.; Solomon, E. I. *Chem. Rev.* **1996**, *96*, 2239−2314.
(15) Rosenzweig, A. C.; Frederick, C. A.; Lippard, S. J.; Nordlund, P. *Nature* **1993**, *366*, 537−543.
(16) Valentine, M.; Lippard, S. J. *J. Chem. Soc., Dalton Trans.* **1997**, 3925−3931.
(17) Que, L. Jr.; Ho R. Y. N. *Chem. Rev.* **1996**, *96*, 2607−2624.
(18) Holm, R. H.; Kennepohl, P.; Solomon, E. I. *Chem. Rev.* **1996**, *96*, 2239−2314.
(19) Wallar, B. J.; Lipscomb, J. D. *Chem. Rev.* **1996**, *96*, 2625−2657.
(20) Feig, A. L.; Lippard, S. J. *Chem. Rev.* **1994**, *94*, 759−805.
(21) Karlin, K. D. *Science* **1993**, *201*, 701−708.
(22) Reedijk, J. *Bioinorganic Catalysis*; Marcel Dekker: New York, 1993.

S0002-7863(98)00006-7 CCC: $15.00
Published on Web 08/29/1998

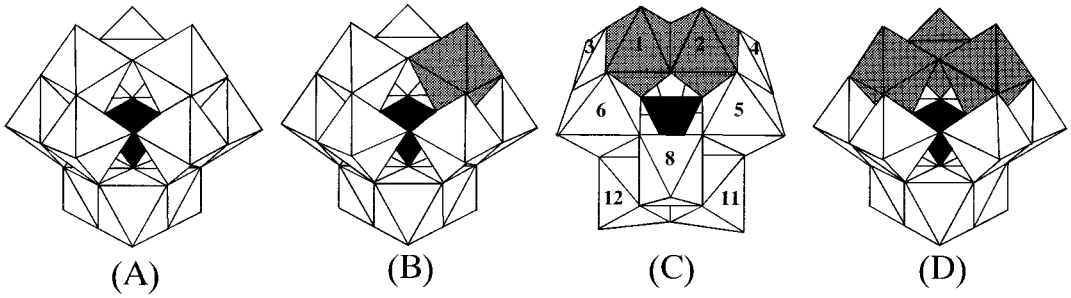

Figure 1. Polyhedral representation of (A) $[\alpha\text{-}SiW_{12}O_{40}]^{4-}$, (B) $[\alpha\text{-}SiW_{11}Fe(OH_2)O_{39}]^{5-}$, (C) $[\gamma\text{-}SiW_{10}\{Fe(OH_2)\}_2O_{38}]^{6-}$ (**I**), and (D) $[\alpha\text{-}SiW_9\{Fe(OH_2)\}_3O_{37}]^{7-}$ Keggin-type polyoxometalates. Iron atoms are represented by shaded octahedra. WO_6 octahedra occupy the white octahedra, and an SiO_4 group is shown as the internal black tetrahedron. The Wn represents the number of WO_6 site in Keggin structure in Figure 1C. The numbering is based on IUPAC recommendations.

While a number of structural models with diiron center have been reported, functional models with diiron center for oxygenations of alkanes are fewer in numbers because of the instability of the catalysts.[32,33] $[Fe(salen)]_2O$ (salen = *N*,*N*-ethylenebis(salicyldeneaminato)), $Fe_2O[HB(pz)_3]_2(OAc)_2$ (pz = 3,5-bis(isopropyl)pyrazolyl), $[(PA)_2Fe]_2O$ (PA = 2,6-dicarboxylatopyridine), $Fe_2O(OAc)_2(bpy)_2Cl_2$ (bpy = 2,2′-bipyridine), and $[Fe_2(TPA)_2O(OAc)](ClO_4)_3$ (TPA = tris(2-pyridylmethyl)-amine) are examples. In contrast, polyoxometalates have an attractive aspect in catalysis, i.e., their inherent stability toward oxygen donors.[34−36]

In this paper, we compare the catalytic activity of mono-, di-, and triiron-substituted polyoxometalates shown in Figure 1 and find that diiron-substituted polyoxometalate can uniquely catalyze the selective oxygenation of alkanes with highly efficient utilization of hydrogen peroxide.

Experimental Section

Preparation of Polyoxometalates. The following polyoxometalates, $[\alpha\text{-}SiW_{12}O_{40}]^{4-}$, $[\alpha\text{-}SiW_{11}Fe(OH_2)O_{39}]^{5-}$, $[\gamma\text{-}SiW_{10}Mn_2O_{38}]^{6-}$, $[\gamma\text{-}SiW_{10}\{Fe(OH_2)\}_2O_{38}]^{6-}$, and $[\alpha\text{-}SiW_9\{Fe(OH_2)\}_3O_{37}]^{7-}$ were synthesized as tetrabutylammonium salts as follows.

$[(C_4H_9)_4N]_4[\alpha\text{-}SiW_{12}O_{40}]$. Tetrabutylammonium salt of $[\alpha\text{-}SiW_{12}O_{40}]^{4-}$ was precipitated by adding an excess amount of $[(C_4H_9)_4N]Br$ (3.48 g, 11 mmol) to $K_4[\alpha\text{-}SiW_{12}O_{40}]\cdot 17H_2O$ (3.0 g, 0.9 mmol) according to the published method.[37] Elemental Anal. Found (calcd) for $[(C_4H_9)_4N]_4[\alpha\text{-}SiW_{12}O_{40}]$: C, 20.15 (20.00); H, 3.55 (3.78); N, 1.54 (1.46). Infrared spectrum (cm^{-1}): 967 (s), 920 (s), 884 (s), 801 (s, br). UV−visible spectrum in acetonitrile at 296 K: λ_{max} = 264 nm (ϵ = 37 200 M^{-1} cm^{-1}). Both spectra were characteristic of α-Keggin structure.

$[(C_4H_9)_4N]_{4.25}H_{0.75}[\alpha\text{-}SiW_{11}\{Fe(OH_2)\}O_{39}]$. $K_5[\alpha\text{-}SiW_{11}\{Fe(OH_2)\}O_{39}]\cdot 14H_2O$ was prepared according to ref 38. The purity of $K_5[\alpha\text{-}SiW_{11}\{Fe(OH_2)\}O_{39}]\cdot 14H_2O$ was checked by infrared (cm^{-1}) (966 (s), 911 (s), 791 (s, br)) and UV−visible (λ_{max} = 259 nm (ϵ = 39 000 M^{-1} cm^{-1})) spectra. The tetrabutylammonium salt of $[\alpha\text{-}SiW_{11}\{Fe(OH_2)\}O_{39}]^{5-}$ was precipitated by adding an excess amount of $[(C_4H_9)_4N]Br$ (4.3 g, 13.3 mmol) to aqueous solution of $K_5[\alpha\text{-}SiW_{11}\{Fe(OH_2)\}O_{39}]\cdot 14H_2O$ (2.5 g, 0.78 mmol). The precipitate was purified by repeated reprecipitation from acetonitrile solution with the addition of excess water. Elemental Anal. Found (calcd) for $[(C_4H_9)_4N]_{4.25}H_{0.75}[\alpha\text{-}SiW_{11}Fe(OH_2)O_{39}]$: C, 21.34 (21.61); H, 4.15 (4.15); N, 1.65 (1.58). Infrared spectrum (cm^{-1}): 966 (s), 911 (s), 791 (s, br) in agreement with those of $K_5[\alpha\text{-}SiW_{11}Fe(OH_2)O_{39}]$. Raman spectrum ($cm^{-1}$): 965 (s), 952 (s), 232 (m), characteristic of α-Keggin structure.[39] UV−visible spectrum in acetonitrile at 296 K: λ = 261 nm (ϵ 47 500 M^{-1} cm^{-1}) and 473 nm (ϵ 19 M^{-1} cm^{-1}).

$[(C_4H_9)_4N]_{3.25}H_{3.75}[\alpha\text{-}SiW_9\{Fe(OH_2)\}_3O_{37}]$. The tetrabutylammonium salt of $[\alpha\text{-}SiW_9\{Fe(OH_2)\}_3O_{37}]^{7-}$ was prepared by adding $[(C_4H_9)_4N]Br$ (16.8 g, 52 mmol) to $[\alpha\text{-}SiW_9\{Fe(OH_2)\}_3O_{37}]^{7-}$ (4.0 mmol) in aqueous solution. The precipitate was purified by repeated reprecipitation from acetonitrile solution with the addition of excess water. Elemental Anal. Found (calcd) for $[(C_4H_9)_4N]_{3.25}H_{3.75}[\alpha\text{-}SiW_9\{Fe(OH_2)\}_3O_{37}]$: C, 18.48 (18.98); H, 3.54 (3.88); N, 1.44 (1.38). Infrared spectrum (cm^{-1}): 966 (s), 912 (s), and 800 (s, br) in agreement with band positions of $K_6H[\alpha\text{-}SiW_9\{Fe(OH_2)\}_3O_{37}]\cdot 8H_2O$.[40] Raman spectrum ($cm^{-1}$): 973 (s), 956 (s), 226 (m), characteristic of α-Keggin structure.[39] UV−visible spectrum in acetonitrile at 296 K: λ = 262 nm (ϵ 38 000 M^{-1} cm^{-1}) and 461 nm (ϵ 39 M^{-1} cm^{-1}).

$[(C_4H_9)_4N]_4H_6[\gamma\text{-}(SiO_4)W_{10}Mn^{III,III}{}_2O_{36}]\cdot 1.5CH_3CN\cdot 2H_2O$. Tetrabutylammonium salt of $[\gamma\text{-}SiW_{10}Mn_2O_{38}]^{6-}$ was prepared according to the published method.[41] Infrared spectrum (cm^{-1}): 958 (s), 911 (s), 897 (s), 792 (s, br). UV−visible spectrum in acetonitrile at 296 K: λ = 284 nm (ϵ 15 800 M^{-1} cm^{-1}) and 348 nm (ϵ 3125 M^{-1} cm^{-1}).

$[(C_4H_9)_4N]_{3.5}H_{2.5}[\gamma\text{-}SiW_{10}\{Fe(OH_2)\}_2O_{38}]\cdot H_2O$[42] (abbreviated by (**I**)). Tetrabutylammonium salt of $[\gamma\text{-}SiW_{10}\{Fe(OH_2)\}_2O_{38}]^{6-}$ was synthesized by modification of the method reported for the $\gamma\text{-}SiW_{10}Mn_2O_{38}{}^{6-}$ polyoxometalate[41] as follows. Stoichiometric amounts of $K_8[\gamma\text{-}SiW_{10}O_{36}]\cdot 12H_2O$ (2.0 g, 1.0 mmol) and $Fe(NO_3)_3\cdot 9H_2O$ (0.82 g, 2.0 mmol) were mixed under acidic condition. After the solution had been stirred for 5 min, the addition of an excess tetrabutylammo-

(23) Kurtz, D. M., Jr. *Chem. Rev.* **1990**, *90*, 585−606.
(24) Fish, R. H.; Konings, M. S.; Oberhausen, K. J.; Fong, R. H.; Yu, W. M.; Christou, G.; Vincent, J. B.; Coggin, D. K.; Bauchanan, R. M. *Inorg. Chem.* **1991**, *30*, 3002−3006.
(25) Rabion, A.; Chen, S.; Wang, J.; Buchanan, R. M.; Seris, J.-L.; Fish, R. H. *J. Am. Chem. Soc.* **1995**, *117*, 12356−12357.
(26) Ménage, S.; Galey, J.-B.; Hussler, G.; Seité, M.; Fontecave, M. *Angew. Chem., Int. Ed. Engl.* **1996**, *35*, 2353−2355.
(27) Rabion, A.; Buchanan, R. M.; Seris, J.-L.; Fish, R. H. *J. Mol. Catal.* **1997**, *116*, 43−47.
(28) Maschmeyer, T.; Oldroyd, R. D.; Sankar, G.; Thomas, J. M.; Shannon, I. J.; Klepetko, J. A.; Masters, A. F.; Beattie, J. K.; Catlow, C. R. A. *Angew. Chem., Int. Ed. Engl.* **1997**, *36*, 1639−1642.
(29) Mukerjee, S.; Stassinopoulos, A.; Caradonna, J. P. *J. Am. Chem. Soc.* **1997**, *119*, 8097−8098.
(30) Kim, C.; Dong, Y.; Que, L., Jr. *J. Am. Chem. Soc.* **1997**, *119*, 3635−3636.
(31) Valentine, A. M.; Wilkinson, B.; Liu, K. E.; Komar-Panicucci, S.; Priestley, N. D.; Williams, P. G.; Morimoto, H.; Floss, H.; Lippard, S. J. *J. Am. Chem. Soc.* **1997**, *119*, 1818−1827.
(32) Leising, R. A.; Kim, J.; Perez, M. A.; Que, L. Jr. *J. Am. Chem. Soc.* **1993**, *115*, 9524−9530.
(33) Sheldon, R. A. *Catalytic Activation and Functionalisation of Light Alkanes*; Kluwer Academic: Dordrecht, The Netherlands, 1998; p. 259−295.
(34) Neumann, R.; Gara, M. *J. Am. Chem. Soc.* **1994**, *116*, 5509−5510.
(35) Pope, M. T.; Müller, A. *Angew. Chem., Int. Ed. Engl.* **1991**, *30*, 34−48.
(36) Zhang, X.; Chen, Q.; Duncan, D. C.; Campana, C. F.; Hill, C. L. *Inorg. Chem.* **1997**, *36*, 4208−4215.
(37) Tézé, A.; Hervé, G.; Pope, M. T. *Inorg. Synth.* **1990**, *27*, 85−96.
(38) Zonnevijlle, F.; Tourné, C. M.; Tourné, G. F. *Inorg. Chem.* **1982**, *21*, 2751−2757.
(39) R.-Deltcheff, C.; Fournier, M.; Franck, R.; Thouvenot, R. *Inorg. Chem.* **1983**, *22*, 207−216.
(40) Liu, J.; Ortéga, F.; Sethuraman, P.; Katsoulis, D. E.; Costello, C. E.; Pope, M. T. *J. Chem. Soc., Dalton Trans.* **1992**, 1901−1906.
(41) Zhang, X.; O'Connor, C. J.; Jameson, G. B.; Pope, M. T. *Inorg. Chem.* **1996**, *35*, 30−34.

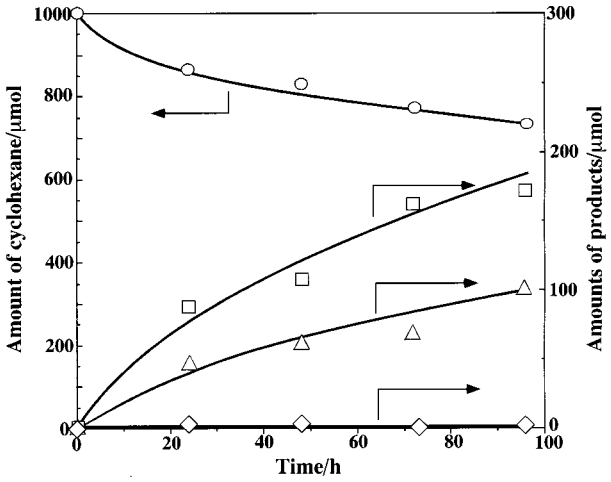

Figure 2. Time course of oxygenation of cyclohexane with hydrogen peroxide catalyzed by **I** in acetonitrile at 305 K. ○, cyclohexane; □, cyclohexanone; △, cyclohexanol; ◇, dicyclohexyl.

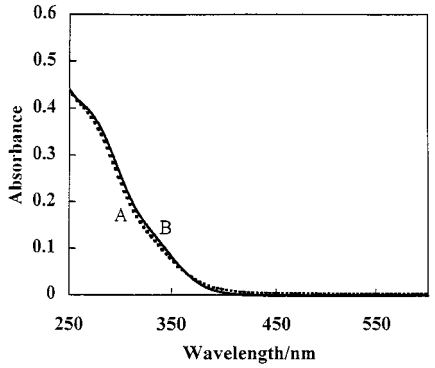

Figure 3. UV−vis spectra of as-prepared and spent **I** (1.3×10^{-2} mM). (A) As-prepared **I** in acetonitrile at 296 K (dotted line). (B) **I** after use for the oxygenation of cyclohexane at 305 K for 96 h (solid line).

nium nitrate (3.1 g, 10 mmol) resulted in a white-yellow precipitate. The precipitate was filtered off and purified by twice dissolving it in acetonitrile (15 mL) and then adding water (300 mL) to reprecipitate the product. The resulting hydrophobic quaternary tetrabutylammonium salt was purified by reprecipitation from acetonitrile/water. The yellow-orange precipitate of tetrabutylammonium salt of $[\gamma\text{-}SiW_{10}Fe_2O_{38}]^{6-}$ is obtained in 37% yield. Elemental Anal. Found (calcd) for $[(C_4H_9)_4N]_{3.5}H_{2.5}[\gamma\text{-}SiW_{10}\{Fe(OH_2)\}_2O_{38}]\cdot H_2O$: C, 19.08 (19.26); H, 3.63 (3.88); N, 1.58 (1.40); Si, 0.80 (0.80); Fe, 3.20 (3.20). Infrared spectrum (cm^{-1}, Figure 4A): 1025 (w), 1002 (w), 961 (s), 903 (s), 886 (s), 797 (s), 755 (s, br), 547 (w) in agreement with those of $[(C_4H_9)_4N]_4H_6[\gamma\text{-}(SiO_4)W_{10}Mn^{III,III}{}_2O_{36}]$. The ^{183}W NMR (11.2 MHz) spectra were referenced to an external standard of the saturated $Na_2WO_4-D_2O$ solution. Chemical shifts were reported on the δ scale with resonances upfield of Na_2WO_4 (δ 0) as negative. The ^{183}W NMR spectrum in acetonitrile at 296 K shows two broad signals at −1334 ($\Delta\nu_{1/2} = 3.1$ kHz) and −1847 ($\Delta\nu_{1/2} = 3.4$ kHz) ppm with integrated intensities of 2:1 (Figure 5A). Two broad signals with integrated intensities of 2:1 were also observed at −1181 and −1700 ppm for the previously known $[\gamma\text{-}SiW_{10}Mn_2{}^{II,II}O_{38}]^{8-}$ polyoxometalate prepared according to ref 41. According to the assignment of Wn in the divanadium-substituted heteropolyanion $[\gamma\text{-}SiW_{10}V_2O_{40}]$,[6−43] the lower field signal is assigned to equivalent W9, W10, W11, and W12 atoms

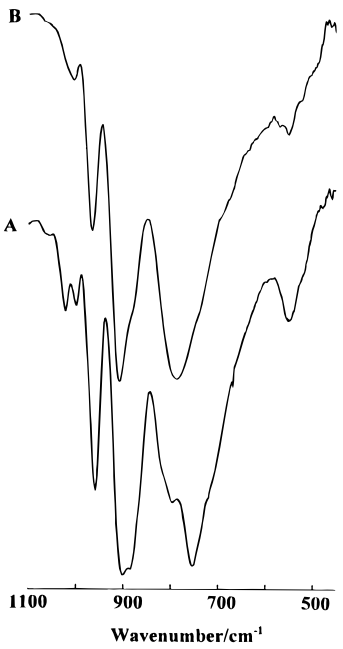

Figure 4. Infrared spectra of as-prepared and spent **I** (KBr disk). (A) As-prepared **I**. (B) **I** after use for the oxygenation of cyclohexane at 305 K for 96 h.

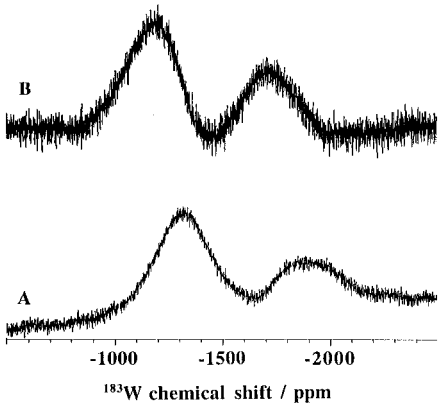

Figure 5. Comparison of ^{183}W NMR spectrum of as-prepared **I** with that after the treatment with H_2O_2. (A) As-prepared **I** in acetonitrile at 296 K (0.15 M) (100 000 transients). (B) 1 equiv of H_2O_2 added to A (after 24 h) (42 240 transients).

and the other signal is assigned to W7 and W8 atoms (Wn, see Figure 1C). The signals due to W3, W4, W5, and W6 atoms bounded to Fe_2O_5 were not observed. The disappearance of signals of W atoms bound to paramagnetic centers has been reported.[44] These facts clearly show that the two iron atoms occupy at 1 and 2 positions. The UV−vis spectrum in acetonitrile at 296 K showed two broad absorption bands at 275 nm (ϵ 22 600 M^{-1} cm^{-1}) and 334 nm (ϵ 10 000 M^{-1} cm^{-1}) (Figure 3A) characteristic of O → W charge-transfer bands of γ-type Keggin structure[45] and one O → Fe charge-transfer band at 470 nm (ϵ 68 M^{-1} cm^{-1}). The negative ion FAB mass spectrum showed no intense peaks in the range of $m/e = -4200$ to −10 000, indicating that $\gamma\text{-}SiW_{10}Fe_2O_{38}{}^{6-}$ is a monomeric compound. The theoretical magnetic moment (spin-only) is 11.0 μ_B for a ferromagnetically coupled $S = 5$ system, and the magnetic moment for this compound is 4.2 μ_B at 296 K, implying some degree of antiferromagnetic coupling. The Mössbauer spectrum at 296 K (isomer shift, 0.32 mm s^{-1}; quadrupole splitting, 0.81 mm s^{-1}) showed that iron ions were equivalent and in high-spin d^5 electronic configuration. All of these facts show the synthesis of the $[\gamma\text{-}SiW_{10}Fe_2{}^{III,III}O_{38}]^{6-}$ polyoxometalate.

(42) Nozaki, C.; Minai, Y.; Kiyoto, I.; Misono, M.; Mizuno, N. Submitted. Our attempts to grow crystallographic quality single crystals of K^+, $(C_4H_9)_4N^+$, $(CN_3H_6)^+$, or $[(CH_3)_3(C_6H_5)N]^+$ salts of $\gamma\text{-}SiW_{10}\{Fe(OH_2)\}_2O_{38}{}^{6-}$ polyoxometalate have been unsuccessful to date; attempts with other cations are in progress.

(43) Canny, J.; Thouvenot, R.; Tézé, A.; Hervé, G.; L.-Loftus, M.; Pope, M. T. *Inorg. Chem.* **1991**, *30*, 976−981.

(44) Lyon, D. K.; Miller, W. K.; Novet, T.; Domaille, P. J.; Evitt, E.; Johnson, D. C.; Finke, R. G. *J. Am. Chem. Soc.* **1991**, *113*, 7209−7221.

(45) Tézé, A.; Canny, J.; Gurban, L.; Thouvenot, R.; Hervé, G. *Inorg. Chem.* **1996**, *35*, 1001−1005.

Table 1. Oxidation of Various Alkanes with Hydrogen Peroxide Catalyzed by **I** at 305 K

substrate	catalyst turnover[a]	conversion[b]/%	product	selectivity/%	H_2O_2 consumed/μmol	efficiency[c]/%
cyclohexane[d]	53	25[e]	cyclohexanol	32[e]	420	99[f]
			cyclohexanone	68[e]		
n-hexane[d]	33	15	hexanols[g]	25	310	83
			hexanones[g]	75		
n-pentane[d]	19	9	pentanols[h]	33	210	74
			pentanones[h]	67		
adamantane[i]	57	42	1-adamantanol	20	460	99
			2-adamantanol	71		
			2-adamantanone	9		

[a] Estimated by moles of oxidizing equivalent in all products per mole of catalyst. [b] (mol of products/mol of substrate used) × 100. [c] ([alcohol] + 2[ketone])/$[H_2O_2]_c$ × 100 (%), where $[H_2O_2]_c$ is the concentration of H_2O_2 consumed. [d] Solvent, acetonitrile, 6 mL; reaction time, 96 h. [e] Conversion and selectivity to oxygenated products. Conversion to dicyclohexyl was <1%. [f] Efficiency to oxygenated products. [g] 1-ol:2-ol:3-ol = 11:35:54; 1-one:2-one:3-one = 0:47:53. [h] 1-ol:2-ol:3-ol = 5:27:68; 1-one:2-one:3-one = 0:35:65. [i] Solvent, acetonitrile/benzene, 6 mL/3 mL; reaction time, 96 h.

Titration of Hydrogen Peroxide. The titration of hydrogen peroxide was carried out according to ref 46. Solution (1−2 g) was accurately weighed and quickly dissolved in 200 mL of water. The solution was stirred with a magnetic stir bar at 296 K. Titration data were obtained with HM-30 pH meter (TOA Electrochemical Measuring Instruments). The potential was monitored as a solution of $Ce(NH_4)_4(SO_4)_4 \cdot 2H_2O$ in water (0.1 M) was added with a buret into the solution in 0.1-mL intervals.

Reaction. Homogeneous reactions of cyclohexane, *n*-hexane, *n*-pentane, and adamantane were carried out in a glass vessel by mixing of 1.0 mmol of substrate, 1.0 mmol of 30% hydrogen peroxide or PhIO, and 8 μmol of polyoxometalate with acetonitrile (6 mL) or acetonitrile (6 mL)/benzene (3 mL) under Ar unless otherwise stated. The reaction solution was periodically sampled and analyzed by gas chromatography on TC-WAX and FFAP capillary columns. For the calculation of the efficiency of hydrogen peroxide utilization, ketones and alcohols were counted as requiring 2 and 1 oxidizing equiv, respectively. The gas-phase analysis was carried out by TCD gas chromatography with Porapak Q and Molecular Sieve 5A columns.

Results and Discussion

The catalytic oxygenation of cyclohexane with hydrogen peroxide was carried out in the presence of **I** for 96 h at 305 K. The time course is shown in Figure 2. The main products were cyclohexanone and cyclohexanol, and no induction period was observed for the formation. The selectivities to cyclohexanone and cyclohexanol changed little with time, showing that the these are the primary products. Only a trace amount of dicyclohexyl, which is formed by the two cyclohexyl radicals, was observed. No acids and oxoesters were observed. It is remarkable that the efficiency of hydrogen peroxide utilization to oxygenated products was almost 100%. The fact that dioxygen was hardly detected in the gas phase supports the finding. Such high efficiency in the oxygenation of cyclohexane has never been reported: For example, the efficiency was higher than those in the cyclohexane oxidations with hydrogen peroxide on the catalysts (efficiency in the parentheses), TS-1 (32%),[8] $[PW_9O_{37}\{Fe_{3-x}Ni_x(OAc)_3\}]^{(9+x)-}$ (x = predominantly 1) (14%),[9] $[Fe_2O(bipy)_4(OH_2)_2][ClO_4]_4$ (8%),[10] $FeCl_3$/py/Ph_2S/picolinic acid system (Gif system, 79%),[11] or $Fe_3O(OAc)_6(H_2O)_3$ (4%).[12] The efficiency was also much higher than those (≤45%) reported for the oxidation of alkenes catalyzed by $[WZnMn_2(ZnW_9O_{34})_2]^{12-}$.[34]

The Keggin-type polyoxometalate isomers and $[SiW_{12-x}\{Fe(OH_2)\}_xO_{40-x}]^{(4+x)-}$ (x = 0−3) polyoxometalates show characteristic UV−vis bands as described partly in the Experimental Section, and therefore, the structures have been often characterized by UV−vis spectroscopy.[38,45,47−49] Figure 3 shows UV−vis spectra of as-prepared and spent **I**, lines A and B respectively. The UV−vis spectrum of **I** after use for the oxygenation reaction showed only the original absorption band with almost the same intensities. As shown in Figure 4B, the IR spectrum of **I** after use for oxygenation reaction showed bands at 1020 (sh), 1007 (w), 967 (s), 908 (s), 876 (sh), 793 (s, br), 736 (sh), and 548 (w) cm^{-1} and the positions are in close agreement with the values for the as-prepared sample shown in Figure 4A. The small change in the signal intensity is probably due to band overlapping or shift by coexisting water, cyclohexanol, and cyclohexanone. The results suggest that **I** is the actual a catalyst. The following results also support the following ideas: (a) When 200 equiv of hydrogen peroxide was added to acetonitrile solution of **I** (0.7 mM) at 296 K, the UV−vis spectrum returned to the original spectrum after the decomposition of hydrogen peroxide. (b) As shown in Figure 5B, the ^{183}W NMR spectrum of **I** showed two broad signals at −1202 ($\Delta\nu_{1/2}$ = 2.6 kHz) and −1704 ($\Delta\nu_{1/2}$ = 2.5 kHz) ppm with integrated intensities 2:1 after **I** was treated with hydrogen peroxide in acetonitrile-d_3 at 296 K. The signal intensities and the ratio were in agreement with those of the as-prepared **I** and the signals appeared in a similar region with the same intensity ratio as that of as-prepared **I**. A little low-field shifts of ^{183}W signals may be caused by the presence of water since it has been reported that the ^{183}W chemical shifts change with solvents.[50,51] A similar high stability has been reported for the sandwich-type polyoxometalates[34,36] and is in marked contrast with the degradation observed for P-containing α-Keggin-type compounds.[52]

Results of oxygenation reactions of *n*-hexane, *n*-pentane, and adamantane catalyzed by **I** are summarized in Table 1. Not only cyclohexane but also *n*-hexane, *n*-pentane, and adamantane were catalytically oxygenated with high efficiency of hydrogen peroxide utilization.

The combination of an iron complex with hydrogen peroxide is often considered to afford Haber−Weiss chemistry,[53] generating hydroxyl radicals that initiate radical autoxidation reactions.[1,24,54] In these reactions alkanes are oxygenated into

(46) Vogel, A. I. *A Textbook of Quantitative Inorganic Analysis Including Elementary Instrumental Analysis*; Longman: New York, 1978.
(47) Tourné, C. M.; Tourné, G. F.; Malik, S. A.; Weakley, T. J. R. *J. Inorg. Nucl. Chem.* **1970**, *32*, 3875−3890.
(48) Peacock, R. D.; Weakley, T. J. R. *J. Chem. Soc. (A)* **1971**, 1937−1940.
(49) Neumann, R.; Vega, M. *J. Mol. Catal.* **1993**, *84*, 93−108.
(50) Nomiya, K.; Nozaki, C.; Miyazawa, K.; Shimizu, Y.; Takayama, T.; Nomura, K. *Bull. Chem. Soc. Jpn.* **1997**, *70*, 1369−1377.
(51) Edlund, D. J.; Saxton, R. J.; Lyon, D. K.; Finke, R. G. *Organometallics* **1988**, *7*, 1692−1704.
(52) Duncan, D. C.; Chambers, R. C.; Hecht, E.; Hill, C. L. *J. Am. Chem. Soc.* **1995**, *117*, 681−691.
(53) Walling, C. *Acc. Chem. Res.* **1975**, *8*, 125−131.
(54) Arends, I. W. C.; Ingold, K. U.; Wayner, D. D. M. *J. Am. Chem. Soc.* **1995**, *117*, 4710−4711.

Table 2. Oxygenation of Alkenes with Hydrogen Peroxide Catalyzed by **I** at 305 K

substrate	conversion[a]/%	product	selectivity[b]/%	H_2O_2 consumed/μmol	efficiency[c]/%
cyclohexene[d]	26	cyclohexene oxide	9(58)	1000	59
		2-cyclohexene-1-ol	18(22)		
		2-cyclohexene-1-one	13(20)		
		1,2-cyclohexanediol	60(0)		
cis-stilbene[e]	23	*cis*-stilbene oxide	34(25)	500	28
		trans-stilbene oxide	11(13)		
		benzaldehyde	31(35)		
		benzyl phenyl ketone	17(11)		
		trans-stilbene	7(16)		
trans-stilbene[e]	18	*trans*-stilbene oxide	66(60)	500	24
		benzaldehyde	34(40)		

[a] Conversion of cyclohexene, C_6(cyclohexene) basis; Conversion of stilbene, C_{14}(stilbene) basis. [b] Numbers in parentheses are selectivities after 1 h. These data are more informative regarding mechanism. [c] See Table 1. [d] Catalyst, 8 μmol; acetonitrile, 6 mL; cyclohexene, 1 mmol; H_2O_2, 1 mmol; reaction time, 96 h. [e] Catalyst, 8 μmol; acetonitrile, 6 mL; substrate, 0.5 mmol; H_2O_2, 0.5 mmol; reaction time, 24 h. Due to the lower solubility of stilbenes than alkanes, the concentrations were decreased, keeping [stilbene]/[H_2O_2] the same as those in Table 1.

Table 3. Oxidation of Cyclohexane with Hydrogen Peroxide Catalyzed by Various Catalysts at 356 K[a]

			selectivity[c]/%			
catalysts	catalyst turnover[b]	conversion[c]/%	cyclohexanol	cyclohexanone	H_2O_2 consumed/μmol	efficiency[d]/%
[γ-$SiW_{10}\{Fe(OH_2)\}_2O_{38}$]$^{6-}$ (**I**)	120	66[e]	55[e]	45[e]	1000	95[e]
[α-$SiW_{11}Fe(OH_2)O_{39}$]$^{5-}$	14	7	42	58	270	41
[α-$SiW_9\{Fe(OH_2)\}_3O_{37}$]$^{7-}$	10	5	48	52	1000	8
[γ-$SiW_{10}Mn_2O_{38}$]$^{6-}$	<2	<1	43	57	1000	<2
[α-$SiW_{12}O_{40}$]$^{4-}$	<2	<1	33	67	120	7

[a] Solvent, acetonitrile, 6 mL; reaction time, 96 h. [b–d] See Table 1. [e] Conversion, selectivity, and efficiency to oxygenated products. Conversion to dicyclohexyl was <1%, and no acids and oxoesters were observed.

alcohols and ketones with the ratio of about 1. The results of cyclohexane, *n*-hexane, and *n*-pentane oxygenation are different from those typically associated from Haber−Weiss chemistry. The results of *n*-hexane, *n*-pentane, and adamantane oxygenation indicate that the reactivity is in the order of $>CH_2 > \gg CH > -CH_3$ and differs from that for radical reactions,[2,55] also suggesting that the nonradical processes prevail to a major degree. The facts that no induction period was observed for the formation of cyclohexanone and cyclohexanol in Figure 2 and that only a trace amount of dicyclohexyl was observed are consistent with the idea.

To provide a evidence for or against nonradical mechanism, oxygenations of alkenes were performed. The results are shown in Table 2. The data for oxygenation of cyclohexene show low selectivity with allylic attack, showing that nonradical processes prevail to a major degree. The epoxidation and oxidative cleavage of aromatic substrates mainly proceeded. The oxidation of *cis*-stilbene with hydrogen peroxide gave *cis*-stilbene oxide, *trans*-stilbene oxide, benzaldehyde, benzylphenyl ketone, and *trans*-stilbene with % selectivities of 34:11:31:17:7, respectively. The approximately 76:24 cis/trans epoxide ratio shows that the present system is more stereospecific than the radical reactions,[54] supporting that nonradical processes prevail to a major degree. The epoxidation of *trans*-stilbene gave *trans*-stilbene oxide and benzaldehyde with % selectivities of 66:34, respectively, in accord with the idea.

The oxygenation of cyclohexane with iodosylbenzene after 96 h gave cyclohexanol with 100% selectivity and 2% conversion. The turnover number and efficiency of iodosylbenzene utilization were 2 and 2%, respectively, and much lower than those for the oxygenation with hydrogen peroxide. The contrast suggests that the oxygenation mechanism is different between two oxidants and that the high-valent iron species, e.g., oxoiron, which has been proposed to be formed by the reaction with iodosylbenzene,[57−59] is not the major iron oxidant species for the oxygenation with hydrogen peroxide.[60]

Table 3 shows the results of cyclohexane oxidation catalyzed by various catalysts obtained at 356 K. Due to the lower activity of the other catalysts, the reaction temperature was increased to 356 K. The time course showed that the conversion and the product yields for **I** did not change after 96 h due to the complete consumption of hydrogen peroxide. The increase in the reaction temperature from 305 to 356 K increased the conversion from 25% to 66% (after 96 h) with only a slight decrease in hydrogen peroxide utilization to 95%. The formation of dioxygen corresponding to ca. 5% hydrogen peroxide decomposition was confirmed. Addition of a second increment of 1000 μmol of hydrogen peroxide to a reacted cyclohexane system[61] resulted in an additional oxygenation (65% conversion and 98% efficiency), showing that the catalyst was not deactivated under the reaction conditions used.

The activity and efficiency for the utilization of hydrogen peroxide greatly depended on the structures of iron centers, and diiron-substituted [γ-$SiW_{10}\{Fe(OH_2)\}_2O_{38}$]$^{6-}$ showed the highest efficiency of hydrogen peroxide utilization and conversion.

(55) Barton, D. H. R.; Csubai, E.; Doller, D.; Ozbalik, N.; Balavoine, G. *Proc. Natl. Acad. Sci. U.S.A.* **1990**, *87*, 3401−3404.

(56) Mizuno, N.; Weiner, H.; Finke, R. G. *J. Mol. Catal.* **1996**, *114*, 15−28.

(57) Smith, J. R. L.; Sleath, P. R. *J. Chem. Soc., Perkin Trans. 2* **1982**, 1009−1015.

(58) Hill, C. L.; Brown, R. B., Jr. *J. Am. Chem. Soc.* **1986**, *108*, 536−538.

(59) Mansuy, D.; Bartoli, J.-F.; Battioni, P.; Lyon, D. K.; Finke, R. G. *J. Am. Chem. Soc.* **1991**, *113*, 7222−7226.

(60) In the present paper, it is not intended to report a detailed analysis of the exact reaction mechanism of the oxygenation process. The additional kinetic, mechanistic, and inhibitor studies are in progress and will be reported in due course.

(61) The oxygenation of cyclohexane was carried out under the following conditions: hydrogen peroxide, 1 mmol; cyclohexane, 2 mmol; **I**, 8 μmol; acetonitrile, 6 mL; reaction temperature, 356 K. The conversion and the efficiency of hydrogen peroxide for the first run (24 h) were 34% and 96%, respectively.

Such a structure dependency of the catalysis is significant, and the catalytic performance of diiron-substituted polyoxometalate may be related to the catalysis by methane monooxygenase[16−23] and Gif system.[55] Dimanganese-substituted [γ-$SiW_{10}Mn_2O_{38}$]$^{6-}$ and *non*-substituted Keggin anion α-$SiW_{12}O_{40}^{4-}$ were inactive. These results show that the diiron site shown in Figure 1C is effective for the oxygenation with hydrogen peroxide.

In conclusion, diiron-substituted polyoxometalate has been shown to catalyze the oxygenation of alkanes at 305 K with very high efficiency of hydrogen peroxide utilization.

Acknowledgment. This work was supported in part by a Grant-in-Aid for Scientific Research from the Ministry of Education, Science, Sports and Culture of Japan.

JA980006C